Single-cell sequencing reveals psilocybin induces sustained cell-type specific plasticity in mouse medial prefrontal cortex

Delong Zhou[1*], Heike Schuler[2*], Vedrana Cvetkovska[1], Juliet Meccia[2], Ashot S. Harutyunyan[3,4], Jiannis Ragoussis[3,4] & Rosemary C. Bagot[1, 5]

[1] Department of Psychology, McGill University, Montréal, QC, Canada
[2] Integrated Program in Neuroscience, McGill University, Montréal, QC, Canada
[3] Department of Human Genetics, McGill University, Montréal, QC, Canada
[4] Victor Phillip Dahdaleh Institute of Genomic Medicine at McGill University, Montréal, Canada
[5] Ludmer Centre for Neuroinformatics and Mental Health, Montréal, QC, Canada
*Authors contributed equally

Corresponding author: Rosemary C. Bagot; rosemary.bagot@mcgill.ca

SUMMARY

The ever-increasing burden of psychiatric disorders and limitations of current treatments have fueled enormous interest in the therapeutic potential of psychedelics. Yet how psychedelics, such as psilocybin, produce lasting therapeutic effects is unclear. Using scRNA-sequencing we identify a type of deep layer near projecting neuron that is most robustly regulated in the medial prefrontal cortex of female mice 24h after psilocybin. We show that this cell-type specificity does not align with 5-HT_{2A} receptor expression but is consistent with the integrated signaling via cell-type specific 5-HT receptor co-expression patterns. Cell-cell communication reveals that psilocybin also broadly suppresses GABAergic inhibition. Ultimately, psilocybin induces plasticity-related genes in subsets of excitatory neurons suggesting that psilocybin induces sustained increases in neuroplasticity in the mouse mPFC. Our findings point to L5/6NP neurons as a key mediator of psilocybin's neuroplastic effects.

INTRODUCTION

In a mounting mental health epidemic, claims that psilocybin, a psychedelic drug, provides lasting relief from a range of psychiatric disorders have fueled an explosion of interest in harnessing its therapeutic potential [1–12]. Psilocybin, a serotonergic hallucinogenic compound produced by fungi, induces both acute and enduring effects[13]. Acutely, psilocybin induces hallucinations and altered states of consciousness[14]. Psilocybin can also induce sustained therapeutic effects in depression and potentially anxiety and alcohol use disorder[1–3,5–7]. Upon ingestion, psilocybin is rapidly metabolized into its active metabolite, psilocin, which ubiquitously binds serotonin receptors[15,16]. While 5-HT_{2A} receptors mediate the hallucinogenic effects[14,17], little is known about the mechanism of psilocybin's sustained effects. Understanding how a single dose of psilocybin can induce lasting effects is critical to support safe and effective clinical use.

Recent findings in rodents and humans point to the medial prefrontal cortex (mPFC) as a locus of psilocybin's therapeutic effects[18–23]. The mPFC mediates higher cognitive functions and is a critical regulator of mood and effects of stress with PFC dysfunction implicated in a range of psychiatric disorders[24,25]. In humans, psilocybin exerts complex effects on prefrontal cortical networks[19,26]. In rodents, psilocybin induces rapid and persistent growth of dendritic spines, increases excitatory neurotransmission, increases BDNF-mTOR signaling and can directly bind the BDNF receptor, TrkB[18,27,28]. However, little is known about the specific cell types that are targeted by psilocybin within the mPFC. Here we used single cell RNA sequencing (scRNAseq) to examine how a single injection of psilocybin enduringly alters gene expression in the mouse mPFC. While technically demanding in brain tissue, scRNAseq offers important advantages over single nucleus RNAseq (snRNAseq). Because snRNAseq is limited to nuclear transcripts, far fewer RNAs are captured, and gene length biases and lack of cytoplasmic RNA species limit inference about RNA in the whole cell[29]. While both methods are powerful in identifying cellular heterogeneity, by capturing cytoplasmic and nuclear RNA, scRNAseq more accurately detects cellular state changes and differential transcriptional regulation[30]. Leveraging single cell transcriptional data to generate cell-type classifiers to predict treatment, algorithms for inferring cell-cell communication and differential gene expression, we reveal that, in female mice, psilocybin preferentially impacts L5/6NP neurons to induce

sustained changes in transcriptional activity consistent with altered network activity. We show that cell-type specific serotonin receptor (5-HTR) distribution suggests that 5-HT_{2A} receptors are not the primary driver of this cell-type specific plasticity, but rather the integrated effects of broad 5-HTR expression.

RESULTS

Psilocybin induces sustained suppression of anxiety-like behavior in female mice

Psilocybin exerts both acute and enduring effects on cognition and behavior in humans and rodents[17,18,31–35]. We first examined the acute dose-response function in male and female mice and confirmed that 1mg/kg maximally increases head-twitch, a field-standard metric for 5-HT_{2A} receptor signaling interpreted as an indicator of the hallucinogenic potential (Figure 1A-C, Table S1)[17]. We then examined the sustained effects, injecting male and female mice with 1 mg/kg psilocybin and testing anxiety-like behavior 24h later in an open field (Figure 1D). While acutely (30 min post injection), 1mg/kg psilocybin similarly increased head twitch in both sexes (Figure 1B, C), 24h later, female, but not male mice, spent significantly more time in the center of an open field, indicating a sustained anxiolytic effect of psilocybin in female mice (Figure 1E, F, Table S2).

Single Cell RNA-Seq reveals L5/6 NP neurons are most strongly targeted by psilocybin

To examine the sustained effect of psilocybin in female mPFC neuronal and non-neuronal cells in female mice, we used scRNA-seq (Figure 1G). Psilocin ubiquitously binds 5-HTRs which are widely expressed so psilocin could impact a range of cell types[15,16,36]. We injected psilocybin, and 24h later dissected mPFC dissociated, captured and sequenced whole cells, retaining 39 435 high-quality cells from 8 independent biological replicates (Figure 1H, Figures S1 A-F, Tables S3). We identified 11 clusters representing all major cell types and many neuron subtypes (Figure 1H), with every neuron subtype represented in all samples (Figure S2E, F, Table S4). We confirmed cluster cell type identity by cell type-specific marker gene expression (Figure 1I, Table S5).

We first asked if the effects of psilocybin are cell-type specific or distributed across a range of cell types. To determine how psilocybin impacted each cell type we used AUGUR[37] for cell type prioritization (Figure 2A). AUGUR builds a classifier for each cell type from a fixed number of cells to predict the treatment condition and then assesses classifier performance on held out cells, with higher scores (area under ROC curves) indicating stronger impact of psilocybin in the cell type. Examining treatment response across cell types revealed a robust response in L5/6 NP neurons, with above chance prediction that exceeded performance of all other cell types (Figure 2B).

We then asked why this specific excitatory neuron subtype is preferentially sensitive to psilocybin. We first considered expression of the gene encoding 5-HT_{2A} receptors, *Htr2a* but found only sparse expression in L5/6NP neurons with highest expression in L2-6 IT neurons and endothelial cells (Figure S2A). To probe the molecular identity of

L5/6 NP neurons we compared gene expression in L5/6 NP neurons to all other excitatory neurons in saline samples and identified 67 genes enriched in L5/6 NP neurons. Among the top three most highly enriched genes, is the gene encoding the 5-HT_{2C} receptor (*Htr2c*) (Figure 2C, Figure S2B,Table S6). We hypothesized that, distinct from the acute hallucinogenic response, sensitivity to psilocybin's sustained effects may be conferred by 5-HT receptor expression patterns beyond the 5-HT_{2A} receptor.

L5/6 NP neurons express distinct complements of 5-HT receptors

To test this, we first mapped serotonin receptor (5-HTR) expression in each neuron type in our scRNA-seq dataset (Figure S2) and then again used AUGUR to predict condition from clusters of neurons subsetted by expression of 5-HTR genes. We hypothesized that, if 5-HTR expression accounted for L5/6 NP sensitivity then sensitivity should be increased by reducing only to cells expressing a specific 5-HTR. However, none of the 5-HTR subsetted classifiers significantly outperformed the L5/6 NP classifier (Table S7) suggesting that expression of any one 5-HTR is unlikely to account for the sensitivity of L5/6 NP to psilocybin.

Individual cells often co-express two or more 5-HTRs such that examining any subtype in isolation may not be indicative of the overall effect of serotonergic signaling at the cell. This is particularly important given that distinct 5-HTR subtypes generally exert excitatory or inhibitory effects on neuronal activity. We therefore examined both expression and co-expression of 5-HTR transcripts in each cell-type to gain insight into cell-type specific transcriptional responses to psilocybin. Because technical dropouts in scRNA-seq data make zero values difficult to interpret, to accurately define co-expression patterns (Figures 2), we used a spatial transcriptomic dataset [38]. Mapping expression of 5-HTRs across neuronal subtypes confirmed that L5/6 NP neurons display uniquely high expression of *Htr2c* and relatively low expression of all other *Htr* transcripts (Figure 2D). In contrast, *Htr2c* expression is low in all other neuronal subtypes, both excitatory and inhibitory.

We then considered the net predicted effect of 5-HTRs in each neuronal subtype. We grouped *Htr* transcripts into either excitatory (*Htr2a, Htr2c, Htr3a, Htr7*) or inhibitory (*Htr1a, Htr1b, Htr5a*) subtypes and plotted the number of cells expressing *only* excitatory or inhibitory transcripts as well as those expressing *both* excitatory and inhibitory transcripts[14,39]. This revealed that L5/6 NP neurons are indeed unique in that a higher fraction of cells express *only* excitatory *Htr* transcripts compared to cells also or only expressing inhibitory *Htr* transcripts (Figure 2E). An opposing pattern characterized all other excitatory neuron subtypes, with a higher fraction of cells expressing *only* inhibitory *Htr* transcripts (Figure 2E). The relative fraction of cells expressing *both* excitatory and inhibitory *Htr* transcripts remains constant at ~ 20% across all neurons (Figure 2E). The observation that high proportions of uniquely excitatory *Htr* expressing cells aligns with high sensitivity to the sustained effect of psilocybin in L5/6 NP neurons suggests the balance of cell-type specific receptor expression as a potential mechanism of cell-type specific sensitivity. The distinct *Htr* expression patterns predict that psilocybin will differentially impact neuron subtypes, exerting a predominantly excitatory effect in L5/6 NP neurons and a predominantly inhibitory effect in other excitatory neurons.

GABAergic neurons display a mixed 5-HTR expression profile predicting mixed effects in inhibitory neurons. Further resolving GABAergic subtypes revealed that heterogeneous *Htr* expression patterns map to specific subtypes with uniquely excitatory *Htr*-expressing cells predominating in *Sncg*$^+$ and *Vip*$^+$ interneurons and uniquely inhibitory *Htr*-expressing cells predominating in *Pvalb*$^+$ and *Sst*$^+$ interneurons. This suggests that effects of psilocybin will be highly cell type specific to interneuron subtypes. Integrating these effects with known interneuron functions and circuit architecture[40] suggests that psilocybin signaling at GABAergic neurons will likely have important effects on network-level neuroplasticity (Figure S3A, B).

Psilocybin suppresses communication from GABAergic neurons

We then asked how the cellular level effects of psilocybin translate into altered cortical network level interactions. We analyzed cell-cell communication using CellChat[41,42] (Figure 3A). CellChat uses a manually curated ligand-receptor interaction database and the scRNA-seq expression matrix to predict cell communication within each treatment condition using network analysis and pattern recognition and identifies alterations in cell-cell communication between conditions. CellChat predicted that psilocybin reduced overall cell-cell communication, and consistent with cell-type prioritization (Figure 2B), this primarily impacted neurons (Figure 3C, D, Table S8), predominantly suppressing communication. Psilocybin also increased Oligodendrocyte communication to other cell types (Figure 3C). As psilocybin altered communication amongst neurons, yet the CellChat method is not optimized for neural communication, we then used NeuronChat, a similar tool that leverages a neuron specific database of inter-neuronal communication that takes into account neurotransmitter signaling[43]. Psilocybin reduced the number of communication pathways from GABAergic neurons to all excitatory neuron subtypes (Figure 3F,G; Table S8). Psilocybin also reduced communication strength from GABAergic neurons to L5/6 NP neurons and increased communication strength among excitatory neurons (Figure S8).

Psilocybin induces synaptic transcriptional programs

To understand more about how psilocybin induces lasting changes, we then probed psilocybin-induced gene expression changes in each cell type. Using a generalized linear mixed model[44] to optimize statistical power while controlling for non-independence of variability (i.e. cells nested within replicates), we identified hundreds of differentially expressed genes (DEGs) across cell-types. Psilocybin regulated the largest number of genes in neurons, consistent with cell-type prioritization and cell-cell communication findings identifying neurons as the primary locus of psilocybin's sustained effect (Figure 4A, Table S6). L5/6 NP neurons contained the largest number of genes upregulated by psilocybin (57) followed by L5 PT neurons (54) with a lower number of downregulated genes in both L5/6 NP (30) and L5 PT (34), again demonstrating that L5/6 NP neurons are most robustly impacted by psilocybin (Figure 2B). In all excitatory neuron subtypes, psilocybin upregulated more genes than it downregulated. GABAergic neurons were unique in having more genes downregulated than upregulated by psilocybin (21 up, 30 down).
To interrogate the biological significance of the sustained transcriptional impact of psilocybin, we used gene set enrichment analysis with clusterProfiler[45], to identify gene ontologies enriched in genes upregulated or downregulated by psilocybin (Table S12-S13). Distilling the resulting large numbers of enriched gene ontologies

to their ancestral terms (Table S13) revealed that psilocybin induced expression of genes associated with nervous system development processes, including regulation of neuron projection development, regulation of vasculature development, regulation of trans-synaptic signaling, and myelination in L5/6 NP neurons (e.g. *Shank3*, *Nrn1*) and, to a lesser degree, inhibitory neurons (e.g. *Myo6*, *Kctd13*) (Figure 4B; Table S12). Psilocybin also increased ribosome biogenesis across excitatory and inhibitory neurons (e.g. *Ubr1* in L5 PT, *Ola1* in L6 CT), and broadly suppressed genes across most cell types (Figure 4B; Table S9-13). Notably, psilocybin also robustly increased expression of immediate early genes (IEGs) in L2-6 IT (e.g. *Arc*, *Nr4a3*) and L6 CT (e.g. *Arc*) and L2-6IT (e.g. *Nr4a3*). The upregulation of IEGs and synaptic genes suggests sustained increases in activity in these cell-types consistent with increased neuroplasticity and altered network activity (Figure 4C).

DISCUSSION

Accumulating evidence suggests that, in addition to acute 5-HT_{2A}-mediated hallucinogenic effects, psilocybin exerts sustained therapeutically relevant neuroplastic effects of unknown mechanism. Here we show that, while acutely, psilocybin similarly induced head twitch response in male and female mice, a single dose of psilocybin induced a delayed reduction in anxiety-like behavior predominantly in female mice. This differential impact of sex on acute and delayed behavioral measures further supports findings suggesting distinct mechanisms mediate the hallucinogenic and neuroplastic effects of psilocybin. We find that the sustained effects of psilocybin are accompanied by cell-type specific transcriptomic changes in mPFC that are most robust in L5/6 NP neurons. This cell-type sensitivity does not align with *Htr2a* expression but is consistent with global *Htr* expression patterns. Inferring cell-cell communication, we find that psilocybin predominantly alters communication between neurons, suppressing GABAergic neuron signaling to all excitatory neurons. Ultimately, we find that psilocybin induces cell-type specific transcriptional programs associated with synaptic plasticity, upregulating synaptic genes in L5/6 NP and GABAergic neurons while increasing activity associated genes in L2-6 IT and L6 CT neurons. Taken together, our findings suggest that integrated 5-HTR signaling mediates acute cell-type specific responses to psilocybin that lead to sustained remodeling of mPFC neuronal network activity.

Cell-type specific transcriptional modulation aligns with cell-type serotonin receptor expression

Using scRNA-sequencing to profile the sustained effects of psilocybin revealed that effects were cell-type specific with L5/6 NP neurons most robustly impacted. To understand why this is so, we analyzed *Htr* expression patterns in MERFISH datasets and discovered that L5/6 NP neurons are unique in predominantly expressing only *Htr2c*, or another 5-HTR gene primarily associated with excitatory effects, and most do not also co-express an inhibitory receptor gene. In contrast, all other excitatory neuron subtypes predominantly express 5-HTR genes associated with inhibitory effects (i.e. *Htr1b* and *Htr1a*) with only a small fraction uniquely expressing excitatory 5-HTR genes. While much research centers on 5-HT_{2A} , psilocin ubiquitously binds 5-HTRs and increasing evidence calls into question the role of 5-HT_{2A} in the therapeutically relevant sustained neuroplastic[18,27,31,46]. We show that cell-type specific patterns of *Htr*

genes predict differential acute effects of psilocybin on cellular activity, increasing L5/6 NP neuron activity, while inhibiting other neurons. Consistent with this prediction, we identify L5/6 NP neurons as the cell-type most robustly transcriptionally regulated by psilocybin.

Single-cell *Htr* gene expression patterns in GABAergic subtypes predict that psilocybin will differentially modulate GABAergic interneuron subtypes. Specifically, *Sst*+ and *Pvalb*+ neurons predominantly express genes encoding inhibitory 5-HTRs, acute inhibition by psilocybin, whereas predominant expression of excitatory 5-HTR genes in *Vip*$^+$ and *Sncg*+ interneurons predicts psilocybin will exert an excitatory effect (Figure S3). This prediction is consistent with an overall reduction in GABAergic signaling to excitatory neurons because *Pvalb*$^+$ and *Sst*$^+$ monosynaptically inhibit excitatory neurons while *Vip*$^+$ interneurons monosynaptically inhibit *Sst*$^+$ *and Pvalb*$^+$ interneurons, ultimately inhibiting the inhibition of excitatory neurons. Integrating *Htr* expression with micro-circuit connectivity, the net predicted impact of psilocybin is therefore decreased GABAergic inhibition of excitatory neurons[40]. Consistent with this prediction, NeuronChat identified reduced GABAergic communication to excitatory neurons and analyzing differential gene expression revealed upregulation of synaptic regulatory genes in GABAergic neurons that are consistent with reduced synaptic function. The top gene upregulated by psilocybin in GABAergic neurons is *Myo6*, a gene encoding an actin-based motor protein implicated in AMPA receptor endocytosis, a process that weakens glutamatergic synaptic strength. Psilocybin also induced *Kctd13,* a gene implicated in regulating synaptic transmission and RhoA signaling[47], and repressed Slitrk3, a gene encoding a synaptic adhesion protein for GABAergic synapse organization[48]. A large body of work implicates *Sst*$^+$ *and Pvalb*$^+$ in mPFC dysfunction in depression and chemogenetically inhibiting *Sst*+ and *Pvalb*+ interneurons in mPFC induces antidepressant effects and increases synaptic plasticity in mice[49]. Broadly, predictions from 5-HTR gene expression patterns, transcriptomically inferred cell-cell communication and differentially regulated genes support that psilocybin suppresses GABAergic function.

Integrating cell-type specific effects of psilocybin points to circuit level modulation

Integrating the acute effects psilocybin, as predicted from 5-HTR gene expression, in increasing activity in L5/6 NP neurons while suppressing both activity in other excitatory neurons and GABAergic function predicts a secondary broad increase in excitatory neuron activity. L5/6 NP neurons primarily have local projection targets, and so increasing activity in these neurons, combined with GABAergic suppression, should propagate neuronal activation across mPFC layers, reigniting activity in excitatory neurons that initially suppressed by psilocybin. In this way, psilocybin may ultimately reset the sensitivity of excitatory neurons to both local and distal excitatory inputs. Broadly consistent with this prediction, we observe increased communication strength among excitatory neurons (Figure S4). Further, *in vivo* and *ex vivo* electrophysiology studies also report that psilocybin induced sustained increases in excitatory synaptic transmission 24h post injection[18].

Intriguingly, a similar pattern of circuit modulation has recently been demonstrated following ketamine, another drug with rapid and sustained anti-depressant effects[50]. In the case of ketamine, one hypothesis of the mechanism of action is that the initial

effects of the drug block NMDARs on GABAergic neurons, suppressing GABAergic function and broadly disinhibiting excitatory networks, to induce a surge in glutamatergic activity and stimulate BDNF release. Extending from our findings suggests that psilocybin may be positioned to exert a similar yet more nuanced effect on network activity, potentially resetting the weights of excitatory networks by acutely increasing activity of local projection neurons while suppressing GABAergic and briefly also suppressing most excitatory neurons. Future work should examine this as a potential circuit mechanism for psilocybin's sustained effects on mPFC network function.

Synaptic and activity-dependent genes identify potential molecular mechanisms of psilocybin's sustained effects

Psilocybin induces sustained increases in synaptic function and structure[18] and our results reveal new insight into molecular mechanisms of these sustained effects. Psilocybin upregulated genes implicated in synaptic plasticity and psychiatric disorders in L5/6 NP and GABA neurons and increased IEG expression in other excitatory neuron subtypes 24h post-injection. In L5/6NP, psilocybin upregulated *Shank3*, a core synaptic scaffold protein implicated in autism spectrum disorders, schizophrenia and anxiety, that is a potential biomarker of antidepressant response[51–53]. Also in L5/6NP, psilocybin upregulated *Nrn1*, an activity dependent regulator of synaptic plasticity that mediates antidepressant-like effects in preclinical models that is induced by BDNF and chronic fluoxetine[54]. In other excitatory neurons, psilocybin upregulated activity associated genes. Notably, psilocybin increased expression of *Arc*, an IEG and cytoskeletal gene implicated in synaptic plasticity and antidepressant response, in both L2-6 IT and L6 CT[55]. In L2-6IT, *Nr4a3*, an IEG implicated in synaptic plasticity and learning, was the gene most strongly upregulated by psilocybin[56]. Both psilocybin and ketamine acutely induce IEG expression in various brain regions[21]. Here we identified sustained activation 24h later, long after psilocybin was fully metabolized, indicating sustained changes in mPFC activity. In L2-6IT, psilocybin increased expression of the AMPA receptor subunit, *Gria1*, and modestly upregulated *Gria1* in L5PT (*logFC* 0.09, *padj* 0.02). This is consistent with reported increases in dendritic spines and excitatory synaptic transmission[18,28]. The modest size of these changes suggests that effects may be limited to subset of neurons, consistent with an observation that only a fraction of spines acutely induced by psilocybin are maintained in a manner that is heterogeneous across neurons[18]. Our data suggest that this regulation may be occurring sparsely across several excitatory neuron subtypes, but likely not in Layer 6 corticothalamic projecting neurons and not in GABA neurons. In addition to relatively restricted regulation of synaptic plasticity genes, we observed broad suppression of mitochondrial genes by psilocybin in neuronal and non-neuronal cells. A recent scRNA-Seq study evaluating the transcriptomic profile of stress vulnerability in mouse mPFC revealed that high stress vulnerability is associated with elevated expression of mitochondrial genes and low expression of synaptic related genes[57]. Taken together, our findings suggest that psilocybin may induce gene expression programs that oppose certain depression-associated transcriptomic signatures.

Here we show that the sustained effect of psilocybin suppresses anxiety-like behavior in female mice and that this is associated with cell-type specific changes in gene expression in the mPFC. Integrating cell-type specific transcriptomic regulation with 5-

HTR gene expression patterns points to a potential circuit mechanism for resetting plasticity in mPFC circuits via suppressing activity in GABAergic and most excitatory neurons while specifically increasing activity in near projecting neurons in L5/6. Profiling differential gene expression we identify potential molecular mediators in glutamatergic and GABAergic neurons of the sustained cell-type specific neuroplastic effects of psilocybin. These findings contribute important new insight into how psilocybin impacts mPFC cell-types and circuits to mediate sustained behavioral changes, and suggest potential circuit and molecular mechanisms for psilocybin's therapeutic efficacy in psychiatric disorders.

RESOURCE AVAILABILITY

Lead Contact

Further information and requests should be directed to the corresponding author, Rosemary C. Bagot (rosemary.bagot@mcgill.ca).

Materials availability

This study did not generate new reagents.

Data & Code Availability

The RNA sequencing data generated in this study have been deposited in the NCBI Gene Expression Omnibus (GEO) repository under accession number GSE283929. The data will be released upon publication of this manuscript. All code used to analyze and visualize the single cell RNA-seq data with pre-processed data can be found in the github repo https://github.com/DelongZHOU/Psilocybin.Female.Mouse.mPFC. The repo will be made public when the manuscript is published.

ACKNOWLEDGEMENTS

Psilocybin was obtained through the Usona Institute's Investigational Drug & Material Supply Program. Usona Institute had no involvement in the study design, funding, execution or interpretation. Some figure elements were made using BioRender. We thank Juan-Pablo Lopez for advice on implementing single-cell preparations in adult brain. We thank Claudia Kleinman for advice on bioinformatic analyses. This work was supported by funding from CQDM, HBHL and the Ludmer Centre for Neuroinformatics and Mental Health. We thank the McGill Genome Centre for technical support.

AUTHOR CONTRIBUTIONS

R.C.B. conceived of the study. D.Z., H.S., V.C., and A.S.H. conducted scRNAseq experiments. D.Z. and H.S. analyzed scRNAseq data. H.S. analyzed MERFISH data. D.Z. conducted and analyzed open field experiments. J.M. conducted and analyzed head twitch experiments. J.R. oversaw scRNAseq capture and sequencing. D.Z., R.C.B., H.S., and V.C. interpreted the results and wrote the manuscript.

DECLARATION OF INTERESTS

During the period of her contribution to this research (2021-2022), J.M. reported receiving consulting fees from Knowde Group inc. and is currently an employee of Usona Institute (2023- present). This employment started after J.M.'s involvement in

the research ended. J.M. approved the final manuscript but was not otherwise involved in the research in any capacity after 2022. No other authors have competing interests to declare.

METHODS

Behavioral Methods

Animals 7-week-old male and female C57BL/6J mice were obtained from Jackson Laboratories and habituated to the colony room for one week prior to the start of manipulations. Animals were maintained on a 12h light-dark cycle (lights on at 7:00am) at 22-25°C group-housed with same-sex cage-mates (5 mice per cage) with *ad libitum* access to food and water. All experimental manipulations occurred during the light cycle, in accordance with guidelines of McGill University's Comparative Medicine and Animal Resources Center and approved by the McGill Animal Care Committee.

Psilocybin injection Psilocybin was obtained from the Usona Institute in Fitchburg, Wisconsin under the Investigational Drug & Material Supply Program. A stock solution was prepared by dissolving psilocybin powder in sterile saline at dilutions of 0.025mg/ml, 0.05mg/ml, 0.1mg/ml and 0.2mg/ml solutions for intraperitoneal injection at 0.01ml/g body weight to probe head-twitch response. To probe sustained effects on open field behavior mice and single-cell sequencing mice were injected with 1mg/kg using 0.1mg/ml psilocybin, then individually placed in a clean cage with a handful of their own home-cage bedding for thirty minutes before being returned to their home cage with cage mates.

Head twitch response Immediately following intraperitoneal injection of vehicle or drug (0.25, 0.5, 1 or 2mg/kg), animals were placed in a clean cage in a behavioral testing room and video recorded under red light for 30 minutes. Video files were then manually analyzed for the number of head twitches exhibited in a 30-minute testing time frame.

Open Field Test Mice were placed in the corner of a 44cm x 44cm white matte acrylic open arena under red light and allowed to freely explore for five minutes. Behavior was recorded, tracked, and quantified using an overhead camera connected to Noldus EthoVisionXT 13 software. Quantification included total time (seconds) spent in the center of the arena (defined as a 27.5cm x 27.5cm central zone) The experiment was performed in two cohorts, and z-scores were calculated within each cohort to account for any cohort-specific variability.

Single Cell RNA-seq Sample Preparation and Sequencing

scRNAseq tissue preparation A separate cohort of female mice were decapitated 24h post saline or psilocybin injection. Brain tissue was dissociated as described in[58]. Brains were extracted, immediately submerged in ice-cold Hibernate-A / B27 / Glutamax medium (HABG; 60 ml of Hibernate A medium with 1 ml of B27 and 0.15 ml of GlutaMAX) and subsequently sliced into 1 mm coronal slices using a cooled brain matrix. Bilateral infralimbic and prelimbic cortices were microdissected in an agarose Petri dish with 2 ml of HABG. Next, the dissected tissue was chopped into small pieces of approximately 0.5 x 0.5 x 0.5 cm and transferred into 5 ml of HABG

supplemented with 45 μM actinomycin. After equilibrating the tissue to 30°C for 8 minutes in a water bath, the tissue was transferred into calcium-free Hibernate-A supplemented with 2 mg ml−1 of papain, 45 μM actinomycin, and 2x GlutaMAX for enzymatic dissociation at 30°C for 30-35 minutes in a shaking water bath (170 rpm).

Following dissociation, the tissue was transferred into 2 ml HABG supplemented with 45 μM actinomycin and equilibrated to RT for 5 minutes. Using fire-polished Pasteur glass pipettes, samples were next mechanically dissociated by triturating suspensions approximately 10 times in 45 seconds. Upon allowing the remaining tissue pieces to settle, the supernatant was passed through a 30 μm filter to remove large debris and cell aggregates. This step was repeated 2 times, until all tissue pieces were dissociated.

To remove any remaining debris, the resulting 6 ml supernatant was carefully layered onto an OptiPrep gradient as described in[59]. Briefly, this gradient sorts cell material into debris and 4 fractions: fraction 1 enriches for oligodendrocytes; fraction 2 enriches for debris; fraction 3 enriches for neurons; fraction 4 enriches for microglia. Following a 15 minute centrifugation (800 g, 4°C), we discarded the debris, fraction 1 and fraction 2; collected fraction 3 in a new tube; and discarded fraction 4. Fraction 3 was then diluted with 5 ml HABG and centrifuged for 3 minutes (200g, 4°C). The supernatant was discarded, and the pellet was resuspended in 5 ml of DPBS supplemented with 0.04% BSA. After a final centrifugation for 3 minutes (200g, 4°C), the supernatant was discarded and the final pellet was resuspended in 50 ul of DPBS supplemented with 0.04% BSA.

scRNA-seq Library Preparation

Single-cell suspensions were washed and resuspended in PBS with 0.04% BSA. We aimed to capture ~8,000 cells per sample. An aliquot of cells was used for LIVE/DEAD viability testing (Thermo Fisher Scientific). Single-cell libraries were generated using the 10x Genomics Chromium Controller or Chromium X instrument and Chromium Next GEM Single Cell 3' GEM, Library & Gel Bead Kit v3.1 (10x Genomics) according to the manufacturer's protocol. Briefly, cells suspended in reverse transcription reagents, along with gel beads, were segregated into aqueous nanoliter-scale gel bead-in-emulsions (GEMs). The GEMs were then reverse transcribed in a T1000 Thermal cycler (Bio-Rad) programed at 53ºC for 45 min, 85ºC for 5 min, and hold at 4ºC. After reverse transcription, single-cell droplets were broken and the single-strand cDNA was isolated and cleaned with Cleanup Mix containing DynaBeads (Thermo Fisher Scientific). cDNA was then amplified with a T1000 Thermal cycler programed at 98ºC for 3 min, 12 cycles of (98ºC for 15 s, 63ºC for 20 s, 72ºC for 1 min), 72ºC for 1 min, and hold at 4ºC. Subsequently, the amplified cDNA was fragmented, end-repaired, A-tailed and index adaptor ligated, with SPRIselect Reagent Kit (Beckman Coulter) with cleanup in between steps. Post-ligation product was amplified with a T1000 Thermal cycler programed at 98ºC for 45 s, 12 cycles of (98ºC for 20 s, 54ºC for 30 s, 72ºC for 20 s), 72ºC for 1 min, and hold at 4ºC. The sequencing-ready libraries were cleaned up with SPRIselect, quality controlled for size distribution and yield (LabChip GX Perkin Elmer), and quantified using qPCR (KAPA Biosystems Library Quantification Kit for Illumina platforms). Libraries were loaded on MGI DNBSEQ-G400 and sequenced using the following parameters: 28 bp Read1, 8

bp Index i7, and 150 bp Read2. Libraries were sequenced at an average depth of 40,000 reads/cell.

scRNA-seq Data Analysis

Pre-processing and quality control CellRanger v7.0.0 was used with option “count” and default parameters to filter and align raw reads to the pre-compiled mouse reference refdata-gex-mm10-2020-A. CellBender v0.3.0 was then used to remove background RNA[60]. Further quality control and processing were performed with Seurat v4.4.0[61]. Cells were filtered on the number of genes (greater than 800 and within two standard deviations from average), the number of total reads (within two standard deviations from average) and mitochondrial content (lower than 10%). In each sample, only genes detected in more than 3 cells were retained. After quality control, two saline-injected samples were pooled due to low cell number.

Identification of cell types Cell type-specific markers were identified by detecting differentially expressed genes between the given cell type and the remaining cells using *FindAllMarkers* function of Seurat[61] package with default parameters. Excitatory neuron sub-type specific markers were identified by detecting differentially expressed genes between the given subtype and the remaining excitatory neurons, thereby excluding markers shared across all excitatory neuron subtypes. SciBet[62], SingleCellNet[63] and SingleR[64] were used to annotate cell types with two published datasets as references. The first dataset consists of cells collected from saline treated P60 animals published by Bhattacherjee, et al[65]. The second dataset consists of cells from the Allen Mouse Brain Atlas with region label ILA;PL;ORB (infralimbic, prelimbic and orbitofrontal areas)[66]. A consensus annotation was assigned when at least two methods agreed. Cells were only assigned as neuron if labeled as neuron by both references. Neuron subtypes were labeled from the Allen Mouse Brain Atlas. The expression of cell type and neuron subtype markers was examined to confirm the cell type assignment.

Normalization, Dimension Reduction and Integration of Samples The dataset was scaled to 10,000 reads per cell and log transformed. Samples were integrated by merging samples without batch correction. Variable features were identified with the variance-stabilizing transform method. Dimension reduction was performed with the 2000 most variable features and the top 30 dimensions were used for clustering and projection to two dimensions with Uniform Manifold Approximation and Projection.

Cell Prioritization Augur[37] was used to probe the magnitude of response of each cell type/subtype to psilocybin injection. A parameter sweep was performed to determine the best combination. The combination of vquant=0.9, ntree=150, mtry=20 optimized prediction and was used for further analysis. The cell condition labels were then shuffled (with Augur "permute" option and otherwise identical parameters as abovementioned) to determine whether the Augur score was significantly above chance.

Identification of Genes Enriched in L5/6NP To identify genes enriched in L5/6NP neurons separate to any effects of psilocybin, L5/6NP enriched genes were identified using only cells from saline samples. The *FindAllMarkers* function of the Seurat package was used with default parameters to compare L5/6NP cells against all remaining excitatory neurons.

Cell-Cell Communication CellChat[41,42] and its associated mouse database were used to estimate cell-cell communication between neuron subtypes and/or non-neuron cell types following the standard pipeline. The numbers of interactions were identified in the control group or psilocybin group separately and were then compared for each combination of source / target cell groups. Given that most differences in cell-cell communication were found in neurons, communications in neurons were further estimated using NeuronChat[43] in a similar manner but with a model and curated database optimized to detect communication between neurons.

Differential Expression Analysis Differential gene expression analysis was performed for each individual cell type with Libra using a negative binomial generalized linear mixed model to account for nesting of cells within biological replicates with offset and Wald test[44]. Genes with absolute Log2 Fold Change greater than 0.1 and adjusted p-value less than 0.05 were considered to be differentially expressed.

Gene Set Enrichment Analysis Gene symbols were first converted to Entrez ID using the DAVID conversion tool (https://david.ncifcrf.gov/helps/conversion.html). Genes without converted Entrez ID were discarded. GSE analysis was then performed using clusterProfiler[67]. To compare ontologies across cell-types, the ancestors of the enriched Gene Ontology terms for each cell-type were obtained using EMBL-EBI's QuickGO REST API (https://www.ebi.ac.uk/QuickGO/api/index.html) and aggregated for the top 50 of either positively or negatively enriched terms in each cell type or subtype.

Serotonin(co-)expression analysis

Spatial transcriptomic MERFISH data[38] from were used to analyse co-expression of HTR receptors in the PL and IL areas. MERFISH data provides more accurate quantification of reads with fewer technical dropouts compared to single-cell RNA sequencing. The increased coverage of GABAergic cell types in this dataset also allowed for a more detailed investigation of HTR expression in these subtypes. The normalized count matrix was downloaded from[38]. For the main analysis, we subset to 7 HTRs, classified as primarily mediating inhibitory (Htr1a, Htr1b, Htr5a) or excitatory effects (Htr2a, Htr2c, Htr3a, Htr7) based on literature[39,68]. For reference, expression levels in all major and GABAergic cell types are shown in Figure S3. UpSet plots were generated on all cells that expressed at least one inhibitory or one excitatory receptor using the *ComplexHeatmap* package in R with the ‘distinct’ setting.

REFERENCES

1. Raison, C. L. *et al.* Single-Dose Psilocybin Treatment for Major Depressive Disorder: A Randomized Clinical Trial. *JAMA* **330**, 843–853 (2023).
2. Davis, A. K. *et al.* Effects of Psilocybin-Assisted Therapy on Major Depressive Disorder: A Randomized Clinical Trial. *JAMA Psychiatry* **78**, 481–489 (2021).
3. Carhart-Harris, R. *et al.* Trial of Psilocybin versus Escitalopram for Depression. *N Engl J Med* **384**, 1402–1411 (2021).
4. Goodwin, G. M. *et al.* Single-Dose Psilocybin for a Treatment-Resistant Episode of Major Depression. *N Engl J Med* **387**, 1637–1648 (2022).

5. von Rotz, R. *et al.* Single-dose psilocybin-assisted therapy in major depressive disorder: A placebo-controlled, double-blind, randomised clinical trial. *EClinicalMedicine* **56**, 101809 (2023).
6. Bogenschutz, M. P. *et al.* Percentage of Heavy Drinking Days Following Psilocybin-Assisted Psychotherapy vs Placebo in the Treatment of Adult Patients With Alcohol Use Disorder: A Randomized Clinical Trial. *JAMA Psychiatry* **79**, 953–962 (2022).
7. Back, A. L. *et al.* Psilocybin Therapy for Clinicians With Symptoms of Depression From Frontline Care During the COVID-19 Pandemic: A Randomized Clinical Trial. *JAMA Netw Open* **7**, e2449026 (2024).
8. Felsch, C. L. & Kuypers, K. P. C. Don't be afraid, try to meditate- potential effects on neural activity and connectivity of psilocybin-assisted mindfulness-based intervention for social anxiety disorder: A systematic review. *Neurosci Biobehav Rev* **139**, 104724 (2022).
9. Ehrmann, K., Allen, J. J. B. & Moreno, F. A. Psilocybin for the Treatment of Obsessive-Compulsive Disorders. *Curr Top Behav Neurosci* **56**, 247–259 (2022).
10. Khan, A. J., Bradley, E., O'Donovan, A. & Woolley, J. Psilocybin for Trauma-Related Disorders. *Curr Top Behav Neurosci* **56**, 319–332 (2022).
11. de Veen, B. T. H., Schellekens, A. F. A., Verheij, M. M. M. & Homberg, J. R. Psilocybin for treating substance use disorders? *Expert Rev Neurother* **17**, 203–212 (2017).
12. Calder, A., Mock, S., Friedli, N., Pasi, P. & Hasler, G. Psychedelics in the treatment of eating disorders: Rationale and potential mechanisms. *Eur Neuropsychopharmacol* **75**, 1–14 (2023).
13. Van Court, R. C. *et al.* Diversity, biology, and history of psilocybin-containing fungi: Suggestions for research and technological development. *Fungal Biol* **126**, 308–319 (2022).
14. Aghajanian, G. Serotonin and Hallucinogens. *Neuropsychopharmacology* **21**, 16S-23S (1999).
15. Meccia, J., Lopez, J. & Bagot, R. C. Probing the antidepressant potential of psilocybin: integrating insight from human research and animal models towards an understanding of neural circuit mechanisms. *Psychopharmacology (Berl)* **240**, 27–40 (2023).
16. Halberstadt, A. L. & Geyer, M. A. Multiple receptors contribute to the behavioral effects of indoleamine hallucinogens. *Neuropharmacology* **61**, 364–381 (2011).
17. Halberstadt, A. L., Chatha, M., Klein, A. K., Wallach, J. & Brandt, S. D. Correlation between the potency of hallucinogens in the mouse head-twitch response assay and their behavioral and subjective effects in other species. *Neuropharmacology* **167**, 107933 (2020).
18. Shao, L.-X. *et al.* Psilocybin induces rapid and persistent growth of dendritic spines in frontal cortex in vivo. *Neuron* **109**, 2535-2544.e4 (2021).
19. Mertens, L. J. *et al.* Therapeutic mechanisms of psilocybin: Changes in amygdala and prefrontal functional connectivity during emotional processing after psilocybin for treatment-resistant depression. *J Psychopharmacol* **34**, 167–180 (2020).
20. Jefsen, O. H., Elfving, B., Wegener, G. & Müller, H. K. Transcriptional regulation in the rat prefrontal cortex and hippocampus after a single administration of psilocybin. *J Psychopharmacol* **35**, 483–493 (2021).
21. Davoudian, P. A., Shao, L.-X. & Kwan, A. C. Shared and Distinct Brain Regions Targeted for Immediate Early Gene Expression by Ketamine and Psilocybin. *ACS Chem Neurosci* **14**, 468–480 (2023).
22. Zhao, X. *et al.* Psilocybin promotes neuroplasticity and induces rapid and sustained antidepressant-like effects in mice. *J Psychopharmacol* **38**, 489–499 (2024).
23. Floris, G., Dabrowski, K. R., Zanda, M. T. & Daws, S. E. Psilocybin reduces heroin seeking behavior and modulates inflammatory gene expression in the nucleus accumbens and prefrontal cortex of male rats. *Mol Psychiatry* (2024) doi:10.1038/s41380-024-02788-y.
24. Pizzagalli, D. A. & Roberts, A. C. Prefrontal cortex and depression. *Neuropsychopharmacology* **47**, 225–246 (2022).

25. Friedman, N. P. & Robbins, T. W. The role of prefrontal cortex in cognitive control and executive function. *Neuropsychopharmacology* **47**, 72–89 (2022).
26. Lee, H. J. *et al.* Psilocybin's Potential Mechanisms in the Treatment of Depression: A Systematic Review. *J Psychoactive Drugs* **56**, 301–315 (2024).
27. Moliner, R. *et al.* Psychedelics promote plasticity by directly binding to BDNF receptor TrkB. *Nat Neurosci* **26**, 1032–1041 (2023).
28. Zhao, X. *et al.* Psilocybin promotes neuroplasticity and induces rapid and sustained antidepressant-like effects in mice. *J Psychopharmacol* **38**, 489–499 (2024).
29. Kim, N., Kang, H., Jo, A., Yoo, S.-A. & Lee, H.-O. Perspectives on single-nucleus RNA sequencing in different cell types and tissues. *J Pathol Transl Med* **57**, 52–59 (2023).
30. Thrupp, N. *et al.* Single-Nucleus RNA-Seq Is Not Suitable for Detection of Microglial Activation Genes in Humans. *Cell Rep* **32**, 108189 (2020).
31. Hesselgrave, N., Troppoli, T. A., Wulff, A. B., Cole, A. B. & Thompson, S. M. Harnessing psilocybin: antidepressant-like behavioral and synaptic actions of psilocybin are independent of 5-HT2R activation in mice. *Proc Natl Acad Sci U S A* **118**, e2022489118 (2021).
32. Carhart-Harris, R. L. *et al.* Psilocybin for treatment-resistant depression: fMRI-measured brain mechanisms. *Sci Rep* **7**, 13187 (2017).
33. Doss, M. K. *et al.* Psilocybin therapy increases cognitive and neural flexibility in patients with major depressive disorder. *Transl Psychiatry* **11**, 574 (2021).
34. Preller, K. H. *et al.* Psilocybin Induces Time-Dependent Changes in Global Functional Connectivity. *Biol Psychiatry* **88**, 197–207 (2020).
35. Nardou, R. *et al.* Psychedelics reopen the social reward learning critical period. *Nature* **618**, 790–798 (2023).
36. Nichols, D. E. Hallucinogens. *Pharmacology & Therapeutics* **101**, 131–181 (2004).
37. Skinnider, M. A. *et al.* Cell type prioritization in single-cell data. *Nat Biotechnol* **39**, 30–34 (2021).
38. Bhattacherjee, A. *et al.* Spatial transcriptomics reveals the distinct organization of mouse prefrontal cortex and neuronal subtypes regulating chronic pain. *Nat Neurosci* **26**, 1880–1893 (2023).
39. Andrade, R. Regulation of membrane excitability in the central nervous system by serotonin receptor subtypes. *Ann N Y Acad Sci* **861**, 190–203 (1998).
40. Pi, H.-J. *et al.* Cortical interneurons that specialize in disinhibitory control. *Nature* **503**, 521–524 (2013).
41. Jin, S. *et al.* Inference and analysis of cell-cell communication using CellChat. *Nat Commun* **12**, 1088 (2021).
42. Jin, S., Plikus, M. V. & Nie, Q. CellChat for systematic analysis of cell-cell communication from single-cell transcriptomics. *Nat Protoc* (2024) doi:10.1038/s41596-024-01045-4.
43. Zhao, W., Johnston, K. G., Ren, H., Xu, X. & Nie, Q. Inferring neuron-neuron communications from single-cell transcriptomics through NeuronChat. *Nat Commun* **14**, 1128 (2023).
44. Squair, J. W. *et al.* Confronting false discoveries in single-cell differential expression. *Nat Commun* **12**, 5692 (2021).
45. Wu, T. *et al.* clusterProfiler 4.0: A universal enrichment tool for interpreting omics data. *Innovation (Camb)* **2**, 100141 (2021).
46. Conn, K. *et al.* Psilocybin restrains activity-based anorexia in female rats by enhancing cognitive flexibility: contributions from 5-HT1A and 5-HT2A receptor mechanisms. *Mol Psychiatry* **29**, 3291–3304 (2024).
47. Escamilla, C. O. *et al.* Kctd13 deletion reduces synaptic transmission via increased RhoA. *Nature* **551**, 227–231 (2017).
48. Takahashi, H. *et al.* Selective control of inhibitory synapse development by Slitrk3-PTPδ trans-synaptic interaction. *Nat Neurosci* **15**, 389–398, S1-2 (2012).
49. Fogaça, M. V. *et al.* Inhibition of GABA interneurons in the mPFC is sufficient and necessary for rapid antidepressant responses. *Mol Psychiatry* **26**, 3277–3291 (2021).

50. Fogaça, M. V., Daher, F. & Picciotto, M. R. Effects of ketamine on GABAergic and glutamatergic activity in the mPFC: biphasic recruitment of GABA function in antidepressant-like responses. *Neuropsychopharmacol.* (2024) doi:10.1038/s41386-024-02002-1.
51. Guilmatre, A., Huguet, G., Delorme, R. & Bourgeron, T. The emerging role of SHANK genes in neuropsychiatric disorders. *Dev Neurobiol* **74**, 113–122 (2014).
52. Song, T.-J. *et al.* Altered Behaviors and Impaired Synaptic Function in a Novel Rat Model With a Complete Shank3 Deletion. *Front Cell Neurosci* **13**, 111 (2019).
53. Ortiz, R. *et al.* Shank3 as a potential biomarker of antidepressant response to ketamine and its neural correlates in bipolar depression. *J Affect Disord* **172**, 307–311 (2015).
54. Alme, M. N., Wibrand, K., Dagestad, G. & Bramham, C. R. Chronic fluoxetine treatment induces brain region-specific upregulation of genes associated with BDNF-induced long-term potentiation. *Neural Plast* **2007**, 26496 (2007).
55. Li, Y. *et al.* A critical evaluation of the activity-regulated cytoskeleton-associated protein (Arc/Arg3.1)'s putative role in regulating dendritic plasticity, cognitive processes, and mood in animal models of depression. *Front Neurosci* **9**, 279 (2015).
56. Hong, H., Su, J., Huang, C., Lu, X. & Cui, Z. Comprehensive insights into the function and molecular and pharmacological regulation of neuron-derived orphan receptor 1, an orphan receptor. *Front Pharmacol* **13**, 981490 (2022).
57. Hing, B. *et al.* Transcriptomic Evaluation of a Stress Vulnerability Network Using Single-Cell RNA Sequencing in Mouse Prefrontal Cortex. *Biol Psychiatry* **96**, 886–899 (2024).
58. Chen, R. *et al.* Decoding molecular and cellular heterogeneity of mouse nucleus accumbens. *Nat Neurosci* **24**, 1757–1771 (2021).
59. Brewer, G. J. & Torricelli, J. R. Isolation and culture of adult neurons and neurospheres. *Nat Protoc* **2**, 1490–1498 (2007).
60. Brewer, G. J. & Torricelli, J. R. Isolation and culture of adult neurons and neurospheres. *Nat Protoc* **2**, 1490–1498 (2007).
61. Hao, Y. *et al.* Integrated analysis of multimodal single-cell data. *Cell* **184**, 3573-3587.e29 (2021).
62. Li, C. *et al.* SciBet as a portable and fast single cell type identifier. *Nat Commun* **11**, 1818 (2020).
63. Tan, Y. & Cahan, P. SingleCellNet: A Computational Tool to Classify Single Cell RNA-Seq Data Across Platforms and Across Species. *Cell Syst* **9**, 207-213.e2 (2019).
64. Aran, D. *et al.* Reference-based analysis of lung single-cell sequencing reveals a transitional profibrotic macrophage. *Nat Immunol* **20**, 163–172 (2019).
65. Bhattacherjee, A. *et al.* Cell type-specific transcriptional programs in mouse prefrontal cortex during adolescence and addiction. *Nat Commun* **10**, 4169 (2019).
66. Yao, Z. *et al.* A taxonomy of transcriptomic cell types across the isocortex and hippocampal formation. *Cell* **184**, 3222-3241.e26 (2021).
67. Wu, T. *et al.* clusterProfiler 4.0: A universal enrichment tool for interpreting omics data. *Innovation (Camb)* **2**, 100141 (2021).
68. Celada, P., Puig, M. V. & Artigas, F. Serotonin modulation of cortical neurons and networks. *Front Integr Neurosci* **7**, 25 (2013).

FIGURES

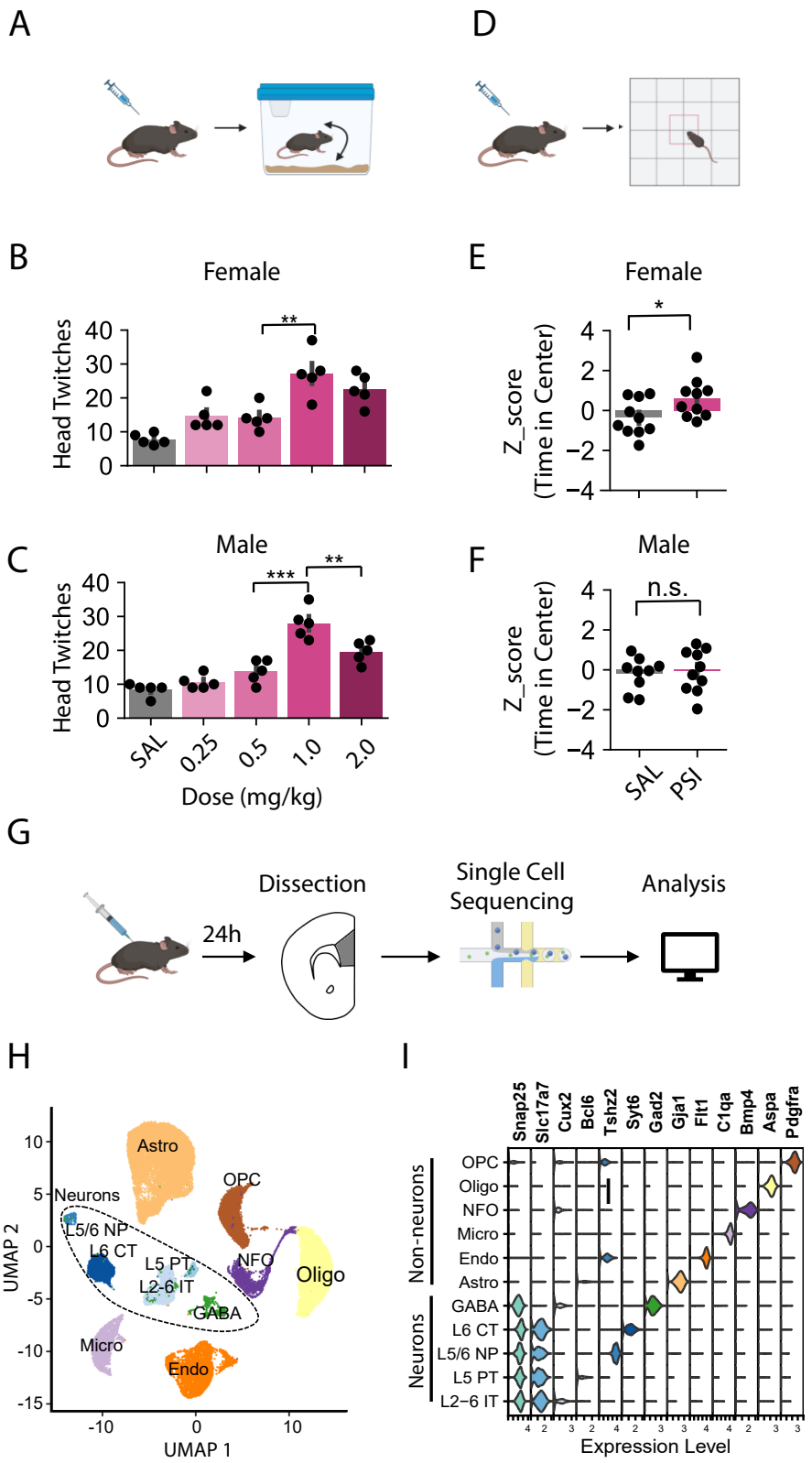
A
D
B
Female
Head Twitches
40
30
20
10
0
**
E
Female
Z_score
(Time in Center)
4
2
0
−2
−4
*
C
Male
Head Twitches
***
**
SAL
0.25
0.5
1.0
2.0
Dose (mg/kg)
F
Male
n.s.
SAL
PSI
G
24h
Dissection
Single Cell
Sequencing
Analysis
H
UMAP 2
UMAP 1
Astro
OPC
Neurons
L5/6 NP
L6 CT
L5 PT
L2-6 IT
NFO
Oligo
GABA
Micro
Endo
I
Snap25
Slc17a7
Cux2
Bcl6
Tshz2
Syt6
Gad2
Gja1
Flt1
C1qa
Bmp4
Aspa
Pdgfra
Non-neurons
Neurons
OPC
Oligo
NFO
Micro
Endo
Astro
GABA
L6 CT
L5/6 NP
L5 PT
L2−6 IT
Expression Level

Figure 1 Behavior & Single Cell RNA-Seq of prefrontal cortex in female mice

(A)Timeline schematic for head-twitch response.

(B)Psilocybin most robustly increases head twitches in female mice at 1.0mg/kg. Effect of treatment $F(4,20)=14.26$, $p<0.0001$, one-way ANOVA; $p=0.002$ between 0.5mg/kg and 1.0mg/kg, Sidak post-hoc tests.

(C) Psilocybin most robustly increases head twitches in male mice at 1.0mg/kg. Effect of treatment $F(4,20)=30.42$, $p<0.0001$, one-way ANOVA; $p<0.001$ between 0.5mg/kg and 1.0mg/kg, $p=0.005$ between 1.0mg/kg and 2.0mg/kg, Sidak post-hoc tests.

(D)Schematic of open field test

(E)24h post-injection, psilocybin injected female mice spend more time in the center of an open field indicating an anxiolytic effect. Two tailed student's t-test, $p=0.03$.

(F) 24h post-injection, there is no difference between psilocybin and saline injected male in center exploration in the open field. Two tailed student's t-test, $p=0.74$.

(G)Schematic of single cell RNA-seq experiment design

(H)UMAP plot showing the clustering of mPFC cell types and neuron subtypes based on transcriptome. Dashed line demarcates neuronal clusters.

(I)Expression of cell type-specific markers in each cell type and neuron subtypes

OPC: oligodendrocyte precursor cell; Oligo: oligodendrocyte; NFO: newly formed oligodendrocyte ; Micro: microglia; Endo: endothelial cell; Astro: astrocyte; GABA: GABAergic neurons; L6CT: Layer 6 corticothalamic neurons; L5/6 NP: Layer 5/6 near projecting neurons; L5 PT: Layer 5 pyramidal tract neurons; L2-6 IT: Layer 2-6 intratelencephalic neurons. B- F, bars represent mean +/- SEM * $p<0.05$, ** $p<0.01$, *** $p<0.001$. Graphics were made using BioRender.

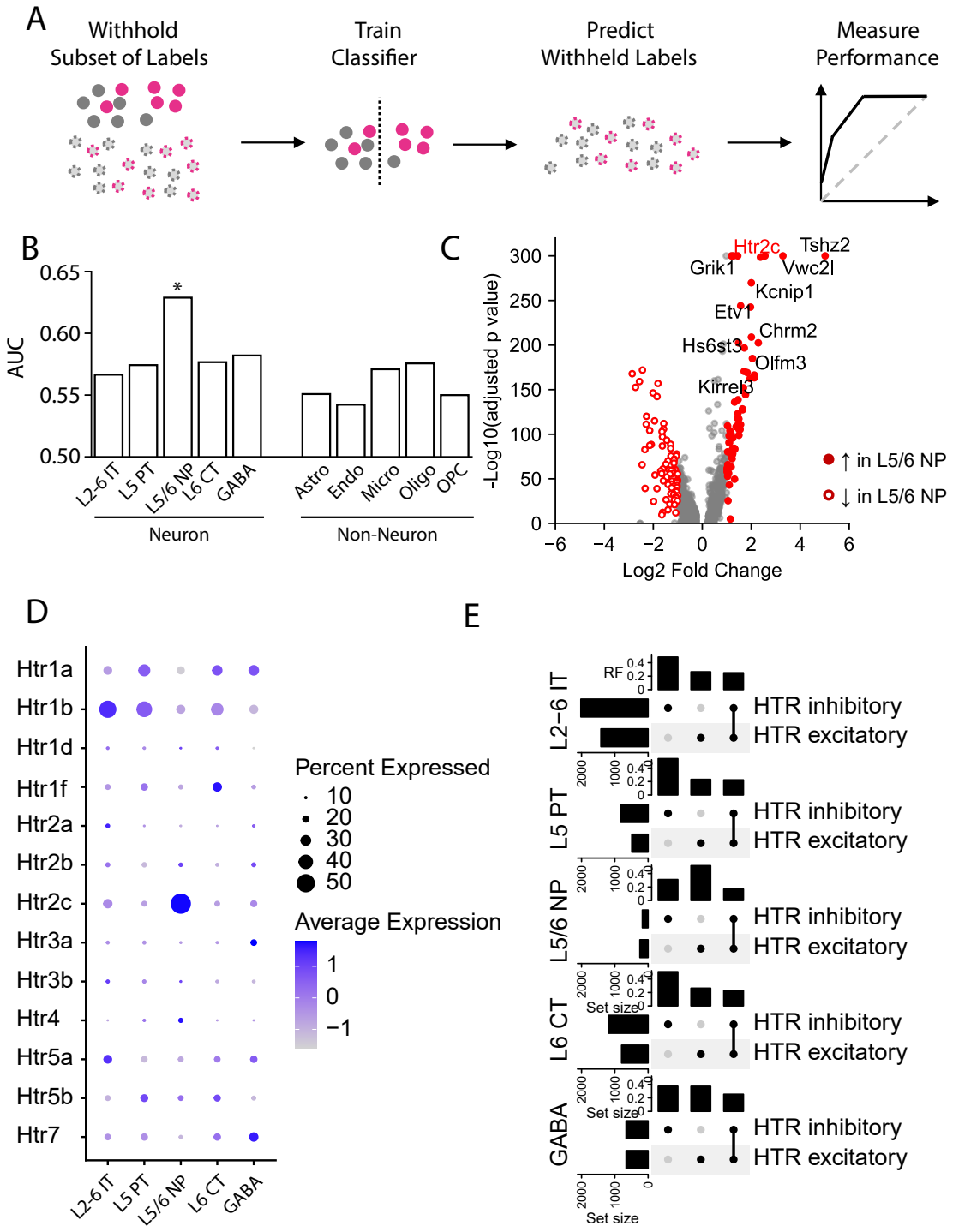

Figure 2 L5/6 NP neurons display the strongest response to psilocybin & unique profiles of 5-HTR genes

(A)Schematic of cell type prioritization with AUGUR[37]

(B)Bar plot depicting AUGUR classifier score (area under the ROC curve) for cell type prioritization. Permutation testing confirmed L5/6 NP predicts treatment effect above

chance (*$p<0.05$). One-way ANOVA confirmed AUC differs across cell types ($F=9.873$, $p= 5.81 \times 10^{-16}$). Post-hoc Tukey's Range Test determined that L5/6 NP prediction exceeds all other cell types (max p.adj= 0.0004).
(C) Volcano plot showing genes that distinguish L5/6 NP from other excitatory neurons. Positive Log2 Fold Change indicates genes with higher expression in L5/6 NP relative to all other excitatory neurons.
(D)Dot plot depicts serotonin receptor expressions in mPFC neuron subtypes measured in spatial transcriptomic data[38].
(E)UpSet plot summarizing cell-type specific gene expression and co-expression of 5-HTR genes in individual cells grouped by 5-HTR category i.e. excitatory (*Htr2a, Htr2c, Htr3a, Htr7*) or inhibitory (*Htr1a, Htr1b, Htr5a*).

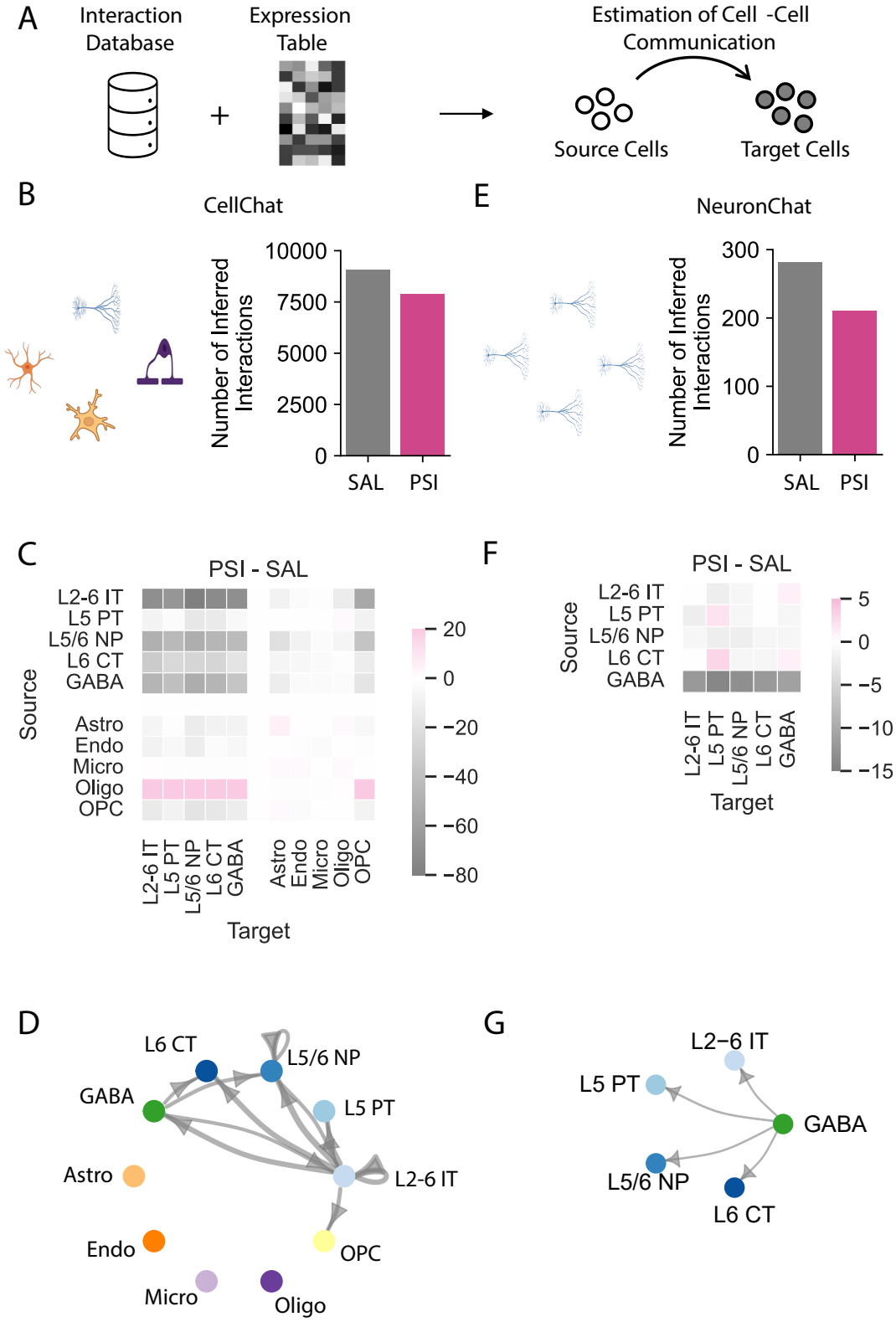

Figure 3. Psilocybin reduces inter-cell communication from GABA neurons
(A)Schematic of cell-cell communication with CellChat[41,42] and NeuronChat.[43]
(B)Bar plot showing the total number of CellChat inferred interactions between all cell types.

(C)Heatmap representing psilocybin induced differences in number of cell-cell communications.
(D)Circle plot depicting the top 10% of differential cell-cell communication induced by psilocybin. Grey edges indicate stronger communication in the saline group relative to psilocybin.
(E)Bar plot showing the total number of NeuronChat inferred interactions between neurons.
(F)Heatmap representing psilocybin induced differences in neuronal communication.
(G)Circle plot showing the top 10% of differential neuron-neuron communication induced by psilocybin. Grey edges indicate stronger communication in the saline group relative to psilocybin.
PSI: psilocybin replicates, SAL: saline replicates. Graphics were made using BioRender.

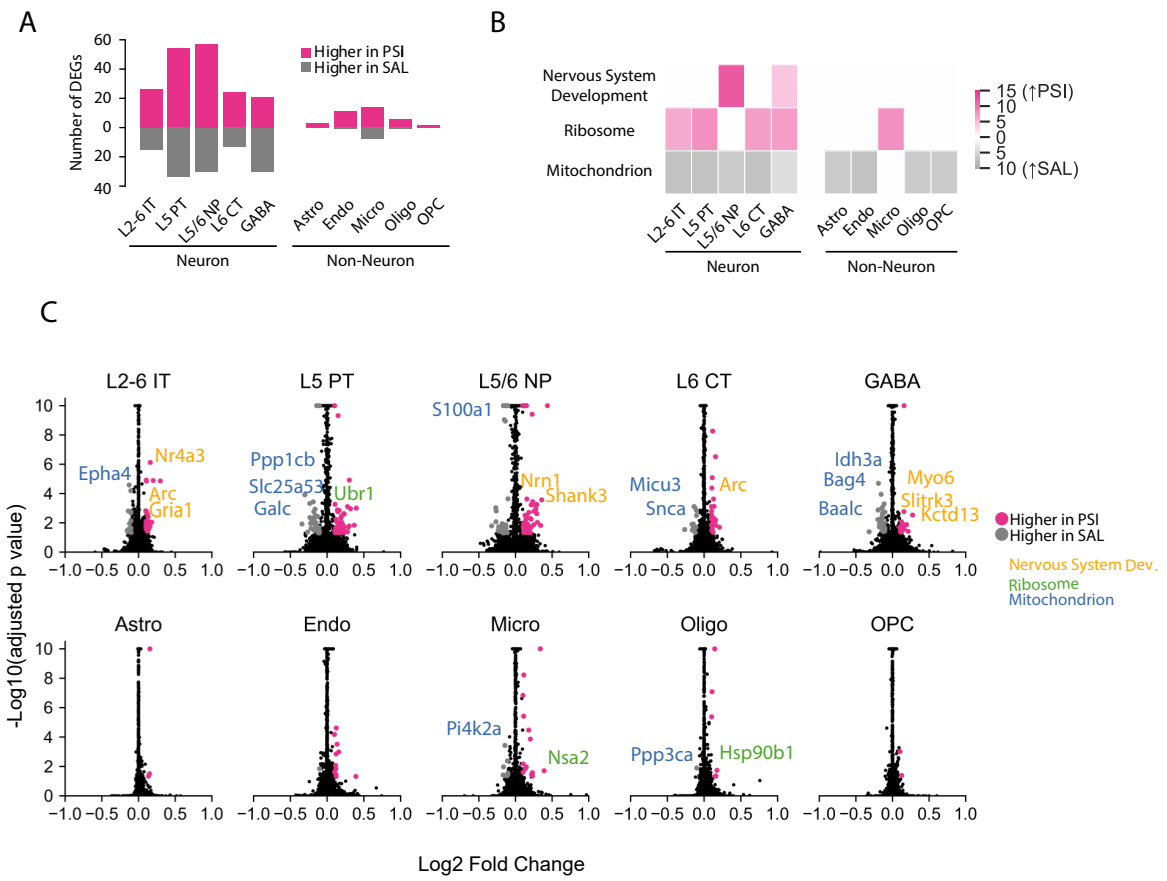

Figure 4. Psilocybin induces cell-type specific gene expression in mPFC
(A)Bar plot shows the number of genes up (pink) or downregulated (grey) by psilocybin in each neuronal and non-neuronal subtype.
(B)Heatmap showing number of Gene Ontology terms grouped by ancestor terms found by GSEA to be enriched in genes up (pink) or downregulated (grey) by psilocybin in each neuronal and non-neuronal subtype.
(C)Volcano plots depict genes significantly up (pink) or downregulated (grey) . Gene name color depicts associated function (orange, nervous system development; blue, mitochondrial; green, ribosomal).